# Tubulation and Aggregation of Spherical Nanoparticles Adsorbed on Vesicles

Amir Houshang Bahrami, Reinhard Lipowsky, and Thomas R. Weikl

*Department of Theory and Bio-Systems, Max Planck Institute of Colloids and Interfaces,*
*Science Park Golm, 14424 Potsdam, Germany*

How nanoparticles interact with biomembranes is central for understanding their bioactivity. In this Letter, we report novel tubular membrane structures induced by adsorbed spherical nanoparticles, which we obtain from energy minimization. The membrane tubules enclose linear aggregates of particles and protrude into the vesicles. The high stability of the particle-filled tubules implies strongly attractive, membrane-mediated interactions between the particles. The tubular structures may provide a new route to encapsulate nanoparticles reversibly in vesicles.

　　　　　　PACS numbers: 87.16.D−, 81.16.Dn, 87.16.af

*Introduction.*—Recent advances in nanotechnology have led to an increasing interest in how nanoparticles interact with biological matter [1]. While biomedically designed nanoparticles are promising carriers in drug treatments [2], the wide application of industrial nanoparticles has also led to concerns about their safety [1,2]. To enter the cells or cell organelles of living organisms, nanoparticles have to cross biomembranes. Therefore, a current focus is on understanding the interactions of nanoparticles with membranes.

Because of their fluidity and softness, biomembranes deform and wrap around nanoparticles if the adhesive interaction between the nanoparticles and membranes is sufficiently strong to compensate for the cost of membrane bending [3,4]. While the wrapping of single nanoparticles by membranes has been studied intensively in theory [3–7] and simulations [8–10], relatively little is known about the organization and the elastic, membrane-mediated interactions of multiple nanoparticles adsorbed on membranes. These interactions arise because the elastic membrane deformations depend on the distance between the adsorbed particles. The elastic pair interactions of rodlike particles with parallel orientation have been found to be repulsive if these particles adsorb to the same side of the membrane [11,12], similar to the pair interactions of inclusions that locally deform the membranes, which are known to be repulsive for rotationally symmetric and equally oriented membrane inclusions [13–16]. More recently, linear aggregates of weakly adsorbed spherical nanoparticles have been observed in simulations and explained by attractive three-particle interactions [17].

In this Letter, we report strongly attractive elastic pair interactions between spherical nanoparticles adsorbed on vesicles. These attractive interactions lead to bound states of the particles with a morphology that depends on the ratio of the area $A$ and volume $V$ of the vesicles. This ratio is typically characterized by the reduced volume $v \equiv 3\sqrt{4\pi}V/A^{3/2} \leq 1$, where the maximal value $v = 1$ corresponds to the area-to-volume ratio of a sphere. For large values of $v$, we find bound states in which two particles are equally wrapped by the vesicle; see Fig. 1(a). For smaller values of $v$, we find even more strongly bound states in which the two particles are jointly wrapped by a membrane tube that invaginates into the vesicle; see Fig. 1(b). For three and more particles, we observe similar bound states in which linear aggregates of the particles are confined within membrane tubes; see Fig. 1(c).

The tubular confinement of linear nanoparticle aggregates reported here constitutes a novel route to encapsulate nanoparticles reversibly in vesicle membranes. The amount of confined nanoparticles as well as their release can be controlled by adjusting the reduced volume of the vesicles, i.e., by deflation and inflation of vesicles via changes in osmotic conditions.

*Model.*—The wrapping and elastic interactions of particles in contact with a vesicle arise from the interplay between membrane bending and adhesion. The total energy is the sum of the bending energy $\mathcal{E}_{be}$ of the vesicle and the overall adhesion energy $\mathcal{E}_{ad}$ of the particles:

$$\mathcal{E} = \mathcal{E}_{be} + \mathcal{E}_{ad}. \tag{1}$$

The bending energy of a homogeneous vesicle without spontaneous curvature is the integral $\mathcal{E}_{be} = 2\kappa \oint M^2 dS$ over the vesicle surface, where $\kappa$ is the bending rigidity of the vesicle membrane and $M$ is the local mean curvature [18]. For a triangulated vesicle surface with $n_v$ vertices, the bending energy $\mathcal{E}_{be}$ can be written as [19]

$$\mathcal{E}_{be} = 2\kappa \sum_{\alpha=1}^{n_v} \frac{M_\alpha^2}{A_\alpha}, \tag{2}$$

where $M_\alpha$ is the mean curvature contribution of the triangulation vertex $\alpha$ and $A_\alpha$ is the area corresponding to the vertex. The mean curvature contribution of vertex $\alpha$ is $M_\alpha = \frac{1}{4}\sum_{\langle ij \rangle} l_{ij} \phi_{ij}$, where the summation extends over all edges $ij$ that share the vertex [19]. Here, $l_{ij}$ denotes the length of the edge, and $\phi_{ij}$ is the angle between the triangles $i$ and $j$ adjacent to the edge. The prefactor $1/4$
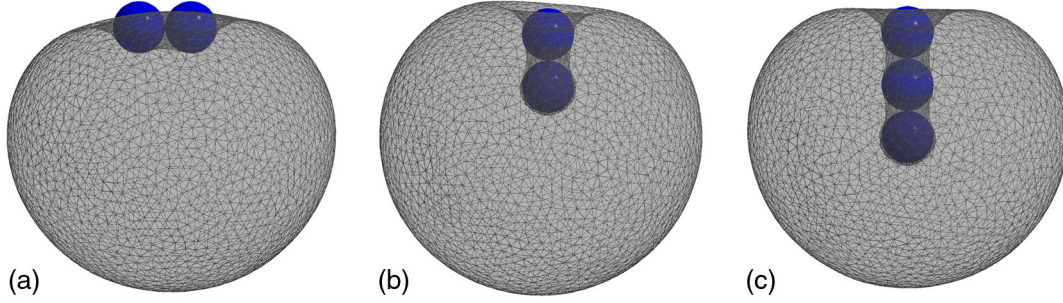
FIG. 1 (color online).   (a) Bound minimum-energy state of two particles for the reduced volume $v = 0.96$ of the vesicle and the rescaled adhesion energy $u \equiv UR_p^2/\kappa = 2$ of the particle, where $U$ is the adhesion energy per area, $R_p$ is the particle radius, and $\kappa$ is the bending rigidity of the vesicle membrane. (b) Bound minimum-energy state of two particles for $v = 0.92$ and $u = 2.33$. (c) Bound state of three particles for $v = 0.88$ and $u = 2$. In (b) and (c), the particles are jointly wrapped by a membrane tube that invaginates into the vesicle.

ensures that the summation over the mean curvature contributions of all vertices tends towards the integral over the mean curvature of the continuous vesicle surface for a large number of vertices [19]. The area corresponding to a vertex is $A_\alpha = \frac{1}{3}\sum_{\langle i \rangle} A_i$, where the sum extends over all triangles $i$ that share the vertex $\alpha$. The prefactor $1/3$ ensures that the summation over all vertices leads to the total area $A = \sum_{\alpha=1}^{n_v} A_\alpha = \sum_{i=1}^{n_t} A_i$ of the triangulated vesicle with $n_v$ vertices and $n_t$ triangles.

The attractive interaction between the particles and the vesicle membrane is described here via a short-ranged square-well interaction potential. A vertex $\alpha$ is bound to a particle with energy $-UA_\alpha$ if the distance of the vertex from the particle surface is within a cutoff distance $d_c$. Here, $U > 0$ is the adhesion energy per area. The total adhesion energy of particles and vesicle then has the form

$$\mathcal{E}_{\text{ad}} = -U\sum_{\langle \alpha \rangle} A_\alpha = -UA_{\text{ad}}, \qquad (3)$$

where the summation extends over all bound vertices and $A_{\text{ad}}$ denotes the total adhesion area of the vesicle.

We determine the minimum total energy $E = \min(\mathcal{E})$ of the vesicle and particles with Monte Carlo simulations and simulated annealing [20]. In our Monte Carlo simulations, the vertices of the triangulated vesicle membrane are displaced to allow changes of the membrane shape, and the edges of the surface are flipped to ensure fluidity within the membrane [21]. The area $A$ and volume $V$ of the vesicle are constrained by harmonic potentials, since the near incompressibility of lipid membranes and the osmotic pressure difference between the vesicle inside and outside lead to constant area and volume [22]. The length of the edges that connect neighboring vertices are kept within an interval $[l, \sqrt{3}l]$ with an edge length $l$ that depends on the number of vertices and the vesicle area [23]. We performed simulations of triangulated vesicles with $n_v = 2562$ vertices and $3 \times 10^7$ Monte Carlo steps per vertex. After initial equilibration, the temperature $T$ is linearly reduced to values close to zero to minimize the total energy $\mathcal{E}$ via a simulated

annealing procedure. The temperature reduction lowers the Metropolis acceptance probability $\exp(-\Delta\mathcal{E}/k_BT)$ for Monte Carlo steps uphill in energy with $\Delta\mathcal{E} > 0$, while steps downhill in energy are always accepted. Here, $\Delta\mathcal{E}$ is the energy difference between the "new" and "old" configurations of a Monte Carlo step. In this simulated annealing procedure, the total energy $\mathcal{E}$ given in Eqs. (1) and (3) is taken to be independent of temperature.

The wrapping and elastic interactions of the particles depend on the reduced volume $v$ of the vesicle, on the rescaled adhesion energy $u = UR_p^2/\kappa$, and on the relative size of the vesicle and particles. We focus here on particles with a radius $R_p = 0.161R_{\text{sp}}$, where $R_{\text{sp}}$ is the radius of a spherically shaped vesicle with reduced volume $v = 1$ in our simulations. The cutoff distance $d_c$ for the attractive square-well interaction between the membrane and the vesicle is chosen to be $d_c = 0.1R_p$.

*Results.*—In Fig. 2, the rescaled total energy $E/\kappa$ of a vesicle with two adsorbed particles is displayed as a function of the particle distance $r$. This energy is obtained from minimization via simulated annealing for fixed distance $r$ of the particles. At the reduced volume $v = 0.96$, the total energy $E(r)$ exhibits local minima at the contact distance $r = 2R_p$ of the particles and at a distance $r$ between $6R_p$ and $9R_p$, separated by an energy barrier. The local minimum of $E$ at the contact distance $r = 2R_p$ corresponds to the bound state of the particles shown in Fig. 1(a) in which both particles are symmetrically wrapped by the vesicle membrane. At the reduced volume $v = 0.92$ and $0.94$, we find additional branches of low-energy conformations with negative values of $E$ at distances $r < 3R_p$ of the particles. In these low-energy conformations, the particles are jointly but asymmetrically wrapped by a membrane tube that invaginates into the vesicles [see Fig. 1(b) and snapshot at the bottom left of Fig. 2]. In these conformations, the wrapping of the particles is asymmetric, since the particle at the tip of the invagination is more strongly wrapped. Besides these low-energy conformations, we find branches of higher-energy conformations with positive values of $E$
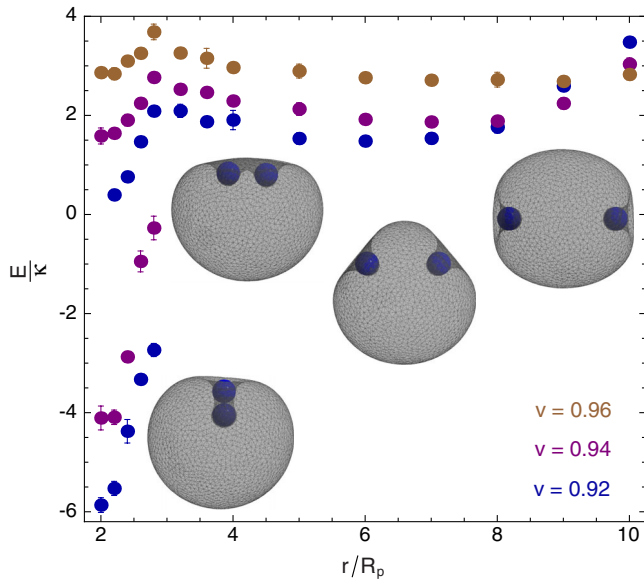
FIG. 2 (color online). Rescaled total energy $E/\kappa$ of a vesicle with two adsorbed particles as a function of the particle distance $r$ for the rescaled adhesion energy $u = 2.33$ and the values $v = 0.92$, 0.94, and 0.96 of the reduced volume. The particles with radius $R_p$ are in contact at the distance $r = 2R_p$. The four snapshots represent minimum-energy conformations for the reduced volume $v = 0.92$ at particle distances with $r/R_p = 2$, 3.2, 6, and 9. Error bars represent the standard deviation of 10 simulations at each rescaled distance.
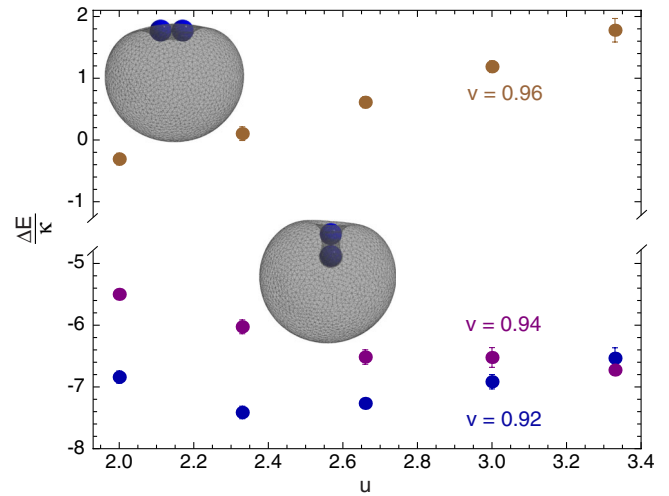


FIG. 3 (color online). Rescaled binding energies $\Delta E/\kappa$ of two adsorbed particles as a function of the rescaled adhesion energy $u$ of the particles. The binding energy $\Delta E$ is calculated as the difference between the total energies $E$ at the particle contact distance $r = 2R_p$ and at the distance $r = 6R_p$, which approximates the location of the second minimum of the interaction profiles $E(r)$ shown in Fig. 2. Negative values of $\Delta E$ correspond to stable bound states of the particles. At the value $v = 0.96$ of the reduced volume, the particles are symmetrically wrapped in their bound states as in the snapshot in the upper left corner. At $v = 0.92$ and 0.94, the particles are bound together by a membrane tube as in the snapshot at the bottom of the figure.

in which the particles are symmetrically wrapped as in Fig. 1(a). The difference in energy between these branches results from a difference in adhesion energy. At $v = 0.92$ and $r = 2.2R_p$, for example, the adhesion energies are $E_{\text{ad}} \simeq -56.7\kappa$ for the low-energy conformation and $E_{\text{ad}} \simeq -51.2\kappa$ for the higher-energy conformation, while the bending energies $E_{\text{be}} \simeq 51.2\kappa$ and $51.6\kappa$ of the two conformations are comparable. These values of $E_{\text{ad}}$ and $E_{\text{be}}$ sum up to total energies $E \simeq 0.4\kappa$ for the higher-energy conformation and $E \simeq -5.5\kappa$ for the low-energy conformation (see Fig. 2).

The binding energy of the two particles can be defined as the energy difference between the two minima in the interaction profiles $E(r)$ of Fig. 2. The binding energies shown in Fig. 3 are calculated as the difference $\Delta E$ between the total energies at the contact distance $r = 2R_p$ and the distance $r = 6R_p$ at which the second minimum is approximately located. At $v = 0.92$ and 0.94, the two particles are strongly bound over the whole range of rescaled adhesion energies $u$ shown in the figure. The binding energies between $-7.5\kappa$ and $-5.5\kappa$ at these values of the reduced volume $v$ are large compared to the thermal energy $k_BT$, since typical values for the bending rigidity $\kappa$ of lipid membranes are of the order of $10 k_BT$. At $v = 0.96$, the particles are stably bound for rescaled adhesion energies $u \lesssim 2$ at which $\Delta E$ is negative. For larger rescaled adhesion energies, we obtain positive values of $\Delta E$.

For three and more adsorbed particles, we obtain strongly bound states in which all particles are confined in a single tube-shaped invagination into the vesicle as depicted in Fig. 1(c). The total energy of these bound states is minimal for particle aggregates that are linear or nearly
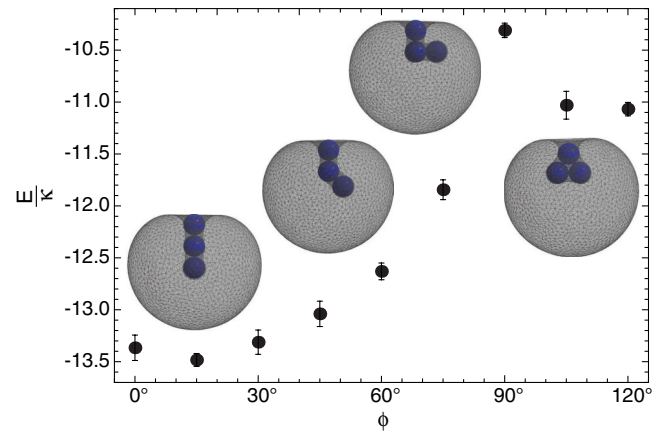


FIG. 4 (color online). Rescaled total energy $E/\kappa$ of a vesicle with three adsorbed particles bound together by membrane tubes as a function of the angle $\phi$ between the particles for the reduced volume $v = 0.88$ and the rescaled adhesion energy $u = 2$. Here, $\phi = 0$ corresponds to a linear arrangement of the particles. The four snapshots depict minimum-energy conformations at the angles $\phi = 0°$, $45°$, $90°$, and $120°$.

linear; see Fig. 4. The minimal total energy $E \simeq -13.5\kappa$ for the strongly bound state of three particles at $\nu = 0.88$ and $u = 2$ is significantly smaller than the energy for other arrangements of the particles. For example, we find a minimum energy of $E \simeq -6.0\kappa$ for configurations in which two of the three particles are bound in a tube and the third particle is adsorbed distant from these two particles.

*Discussion and conclusions.*—The reduced volume $\nu$ is an important parameter to control the number and arrangement of the adsorbed particles. For the relative size of the particles considered here, we find stable membrane tubes with two bound particles at $\nu = 0.92$ and 0.94, but not at $\nu = 0.96$, since the area-to-volume ratio of the vesicle impedes the formation of a membrane tube at this value of the reduced volume (see Fig. 2). For smaller values of $\nu$, we find membrane tubes with three or more bound particles. The membrane tubes are highly stable if the reduced volume $\nu$ is small enough to allow for their formation, with a total energy that depends rather weakly on $\nu$. For example, for three particles that are bound in linear arrangement in a membrane tube as in Fig. 1(c), we obtain the total energies $E \simeq -13.1\kappa$ at $\nu = 0.87$, $E \simeq -13.4\kappa$ at $\nu = 0.88$, and $E \simeq -13.2\kappa$ at $\nu = 0.89$ for the rescaled adhesion energy $u = 2$. For a membrane tube with four particles in linear arrangement, we obtain $E \simeq -28.4\kappa$ at the same value $u = 2$ of the rescaled adhesion energy and values of the reduced volume around $\nu = 0.84$. For a membrane tube with two particles as in Fig. 1(b), we obtain $E \simeq 2.0\kappa$ at $u = 2$ and $\nu = 0.92$. Adding a single particle to the membrane tube for a sufficiently low value of $\nu$ thus reduces the total energy by about $-15\kappa$ at the rescaled adhesion energy $u = 2$. These tube states are significantly more stable than states in which single particles are fully wrapped by the vesicle membrane. At $u = 2$, a fully wrapped particle is only marginally stable, since the bending energy $8\pi\kappa$ of its spherical membrane envelope equals the total adhesion energy $4\pi R_p^2 U$ at this value of the rescaled adhesion energy $u \equiv U R_p^2 / \kappa$ [3,4].

Our tubular membrane structures provide a novel route to confine nanoparticles reversibly in lipid vesicles. The confinement of the particles can be induced by deflating lipid vesicles via changes in the osmotic conditions, and the release of the particles can be triggered by subsequent vesicle inflation. The tubular structures reported here are induced by the adsorbed particles and, thus, have a different origin from similar membrane structures that arise from protein coats [24], from antimicrobial peptides [25], or from aqueous phase separation inside vesicles [26].

The high stability of the deeply wrapped linear aggregates of particles inside the membrane tubes implies strongly attractive elastic interactions that are mediated by the vesicle membrane. In addition, we find attractive interactions between partially wrapped particles for small values $u \lesssim 2$ of the rescaled adhesion energy and high

values of the reduced volume $\nu$ that prevent deeper wrapping and nanotube formation (see the data for $\nu = 0.96$ in Fig. 3). These interactions may help to understand the experimentally observed attractive pair interaction and aggregation of partially wrapped spherical particles on vesicles [27]. In the experiments, the reduced adhesion energy of the particles presumably did not exceed values around $u \simeq 2$, since larger values would lead to full wrapping (see Refs. [3,4] and above). In contrast to the spherical particles considered here, the elastic interactions between membrane-adsorbed rodlike particles with parallel orientation [11,12] and between conical membrane inclusions [13–16] have been found to be repulsive. Membrane shape fluctuations can induce additional attractive interactions between adsorbed particles, since the particles suppress such fluctuations in their adhesion zones. However, these fluctuation-induced interactions are rather weak compared to the elastic interactions reported here [13,28–30].

*Note added.*—In independent work, Saric and Caciutto report tubular membrane structures that are induced by nanoparticles confined within vesicles and discuss these structures in the context of endocytic budding processes [31]. The membrane tubes considered in Ref. [31] protrude out of the vesicles, and these vesicles can freely adapt their volume. In contrast, we treat the vesicle volume as a control parameter, which is experimentally determined by the osmotic conditions, and obtain tubes that protrude into the vesicles and can, thus, store and release nanoparticles in a reversible manner.

[1] A. E. Nel, L. Mädler, D. Velegol, T. Xia, E. M. V. Hoek, P. Somasundaran, F. Klaessig, V. Castranova, and M. Thompson, Nature Mater. **8**, 543 (2009).
[2] W. H. De Jong and P. J. A. Borm, Int. J. Nanomed. **3**, 133 (2008).
[3] R. Lipowsky and H. G. Döbereiner, Europhys. Lett. **43**, 219 (1998).
[4] M. Deserno, Phys. Rev. E **69**, 031903 (2004).
[5] W. T. Gozdz, Langmuir **23**, 5665 (2007).
[6] X. Yi, X. Shi, and H. Gao, Phys. Rev. Lett. **107**, 098101 (2011).
[7] S. Cao, G. Wei, and J. Z. Y. Chen, Phys. Rev. E **84**, 050901 (2011).
[8] H. Noguchi and M. Takasu, Biophys. J. **83**, 299 (2002).
[9] Y. Li and N. Gu, J. Phys. Chem. B **114**, 2749 (2010).
[10] R. Vacha, F. J. Martinez-Veracoechea, and D. Frenkel, Nano Lett. **11**, 5391 (2011).
[11] T. R. Weikl, Eur. Phys. J. E **12**, 265 (2003).
[12] M. M. Mueller, M. Deserno, and J. Guven, Phys. Rev. E **76**, 011921 (2007).

[13] M. Goulian, R. Bruinsma, and P. Pincus, Europhys. Lett. **22**, 145 (1993).

[14] T. R. Weikl, M. M. Kozlov, and W. Helfrich, Phys. Rev. E **57**, 6988 (1998).

[15] P. Dommersnes, J. Fournier, and P. Galatola, Europhys. Lett. **42**, 233 (1998).

[16] B. J. Reynwar and M. Deserno, Soft Matter **7**, 8567 (2011).

[17] A. Saric and A. Cacciuto, Phys. Rev. Lett. **108**, 118101 (2012).

[18] W. Helfrich, Z. Naturforsch. C **28**, 693 (1973).

[19] F. Jülicher, J. Phys. II (France) **6**, 1797 (1996).

[20] S. Kirkpatrick, C. D. Gelatt, Jr., and M. P. Vecchi, Science **220**, 671 (1983)

[21] G. Gompper and D. Kroll, J. Phys. Condens. Matter **9**, 8795 (1997).

[22] R. Lipowsky, M. Brinkmann, R. Dimova, T. Franke, J. Kierfeld, and X. Zhang, J. Phys. Condens. Matter **17**, S537 (2005).

[23] P. S. Kumar and M. Rao, Mol. Cryst. Liq. Cryst. **288**, 105 (1996).

[24] A. Frost, R. Perera, A. Roux, K. Spasov, O. Destaing, E. H. Egelman, P. De Camilli, and V. M. Unger, Cell **132**, 807 (2008).

[25] Y. A. Domanov and P. K. J. Kinnunen, Biophys. J. **91**, 4427 (2006).

[26] Y. Li, R. Lipowsky, and R. Dimova, Proc. Natl. Acad. Sci. U.S.A. **108**, 4731 (2011).

[27] I. Koltover, J. Rädler, and C. Safinya, Phys. Rev. Lett. **82**, 1991 (1999).

[28] R. Golestanian, M. Goulian, and M. Kardar, Phys. Rev. E **54**, 6725 (1996).

[29] T. R. Weikl, Europhys. Lett. **54**, 547 (2001).

[30] H.-K. Lin, R. Zandi, U. Mohideen, and L. P. Pryadko, Phys. Rev. Lett. **107**, 228104 (2011).

[31] A. Saric and A. Cacciuto, preceding Letter, Phys. Rev. Lett. **109**, 188101 (2012)